International Journal of GEOMATE, Oct., 2022, Vol.23, Issue 98, pp.155-163
ISSN: 2186-2982 (P), 2186-2990 (O), Japan, DOI: https://doi.org/10.21660/2022.98.3526
Geotechnique, Construction Materials and Environment

FIELD TEST AND NUMERICAL SIMULATION OF A-FRAME BLADE PILE SYSTEM IN SOLAR FARM

Lin Li[1], Guowei Sui[1], Runshen Wang[1], *Jialin Zhou[1,2] and Erwin Oh[1]

[1]School of Engineering and Build Environment, Griffith University, Australia, [2]Blade Pile Group Pty. Ltd, Australia

*Corresponding Author, Received: 21 July 2022, Revised: 26 Sept. 2022, Accepted: 10 Oct. 2022

ABSTRACT: This paper presents the results of field tests of a designed A-frame blade pile system that is used for resisting lateral wind load action in a solar farm project. The developed system contains an A-frame and two blade piles connected by bolts. The design of A-frame leg-to-ground angle is provided, and a cyclic load test was performed to research the ultimate failure criteria. By data interpretation after testing, it is found that two blade piles have different loading capacities. The reason is that these two piles' mechanical behaviour is different. In detail, one pile is subjected to the "pull out" action, whereas the other pile is subjected to the "push in" effect. Further, the mechanical behaviour of soil is found in this research. The FEM result provided very close behaviour of soil and A-frame blade pile system. Based on the onsite test data and FEM data analysis, the FEM model can provide conservative results. Lastly, the ultimate capacity of this newly developed A-frame blade pile system is defined.

Keywords: A-frame blade pile system; Lateral blade pile capacity; Lateral load; Field Test; FEM Simulation.

1. INTRODUCTION

A pile foundation can be categorized based on the piling technique and its effect on soil, therefore, the Australian standard categorized the pile into two general groups, which are displacement piles as well as non-displacement piles. Some of the other textbooks [1] or reports [2] provide the pile loading conditions, so the classification of the pile can be generally categorized into compressive, uplift, horizontal, and combination loaded piles.

When a pile is subjected to the compression load transferred from the upper structure, the pile shaft and tip cooperated with the soil, and make the contribution to the resistance of the load action. Some structure also transfers the uplift force onto the pier, the capacity of these piers is primarily related to the shaft resistance between the shaft and tip of the pile (related to the soil strength parameter) as well as pile geometry. Other loads such as negative environmental loads (e.g., ocean storms) can create potential hazards for the structure, which may disturb the subsea soil resulting in structural instability [3].

By adding the helix on the pile near the tip of the pile, the pile end area is increased, so this enlarged end pile will increase the compression as well as uplift capacity. The helix piles, also known as blade piles, have been used for a couple of decades, and several blades can be installed along the shaft. When numerous helices are being used, the mechanisms of the soil and blade pile may be different. As Perko [4] pointed out that each individual helix should be considered when they are not close; on the contrary, the cylinder volume between the extreme top and bottom helix should be considered when the distance between the helix is small.

Many previous studies have investigated the helix pile behavior in terms of vertically loaded. the previous research about the individual and cylindrical methods is introduced by [5], [6] and [7],, respectively. The design and analysis methods under vertical load conditions have been conducted very well and can be found in the review by [8] and by [9].

For the blade piles in lateral loads, there is very limited theory provided for the blade pile foundation. Recently, field tests of screw anchor piles were performed, and the interesting found was that the lateral bearing capacity varied over a small range for various soil conditions as well as screw configurations [10]. They also pointed out that there was no suitable method to estimate the helix pile capacity in terms of lateral loads.

A large portion of global energy will come from photovoltaic power, which has become one of the major global energy sources [11]. Solar energy has become one of the cheapest modes of green energy generation in recent years, and the array of piers used in the solar farm may severely be damaged by wind load because the solar panel area encountered with wind is very large. The damage examples recently include array failure at Bhadla Rajasthan, India in terms of uplift and lateral failure in 2019; interior and exterior array failure at Gunma, Japan in terms of uplift and suction, in 2015 [12].

The research of solar panel pier in relation to

uplift loads caused by wind load is studied by experimental tests [13], however, the investigation of the helix pile or blade piles that are used in the solar farm for wind lateral load resistance is rare to found. In this context, this paper focus on the onsite test and FEM simulation of blade pile which is used in solar farm project, and the lateral wind load are considered.

2. RESEARCH SIGNIFICANCE

Due to the natural environment such as wind and earthquakes, ordinary pile foundations can no longer meet the demand. A-frame blade pile systems can provide more load-bearing capacity compared to ordinary pile foundations, which can make the structure more stable. Further, A-frame blade pile system is controlled through a link structure, which allows the solar panels to receive direct sunlight and allows the solar panels to capture the maximum amount of energy. Therefore, it is necessary to study the A-frame blade pile system.

3. A-FRAME BLADE PILE SYSTEM

Figure 1 illustrates the traditional H-beam pile used for resisting the lateral loads induced by wind. In this figure, the load transferred to the pile will be resisted by the soil contact with a flange. Sometimes, for the solar pier design by the engineer, the shaft dimension or pier length should be increased dramatically when the project soil is problematic.

In this context, the material will cost too much when using a large cross-section pier. Therefore, a system that consists of two blade piles that are connected by one frame is designed.

Fig. 1 Traditional H-Beam Pile Solar System (Nextracker Pty Ltd).

The frame which connects two blade piles shall be bent, and the angles between the frame leg and ground are considered from 50 degrees to 90 degrees as shown in Figure 2. As shown in this figure, the minimum length of piles is 1.3 meters with 1-meter embedment, this A-frame blade pile system is designed to be 1.5 m in total height above the ground.

A total of eight FEM models are simulated by using the same material, strength parameters, and geotechnical condition, the only difference among these models is the frame leg-to-ground angles, the minimum and maximum of 50-to-90-degree frames are labelled as An50 to An90, respectively. Note that, An50 is used as an initial model, and several models are made in succession later, which are in increments of 5 degrees.

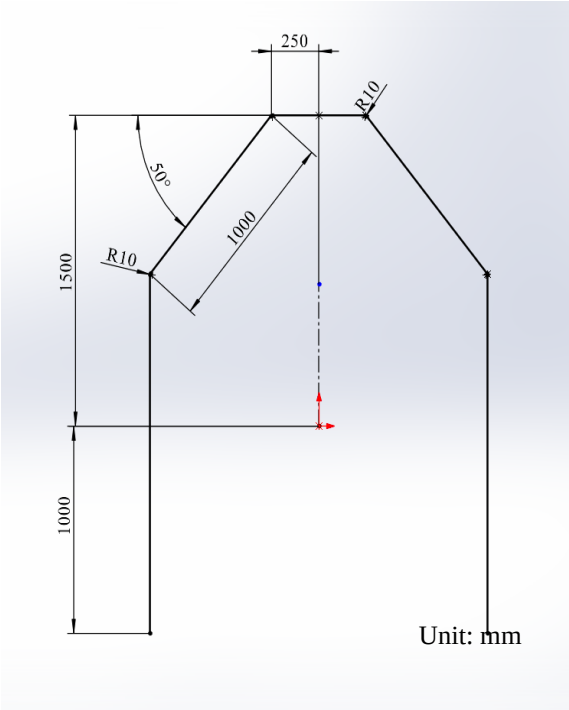

Fig. 2 Frame to Ground Angle Design of System.

Based on the premise that all FEM modelled soils exhibit similar trends. Take the An55 model for example, as shown in Figure 3, when lateral loads are applied from the top of the system, it will be transferred to the soil. In detail, after lateral load (from left to right) is applied, the soil near the pile's top from the right side resists the pile's lateral movement. Also, this figure shows uplift action on the left pile and compressive effect on the right pile.

Furthermore, as shown in Figure 3, the soil above the blades (left blade pile) shows larger stress than the nearby area. Also, for the right-side blade pile, the soil below the blades as well as the soil beneath the tube tip shows larger stress. Compared to the conventional pile design, this load transfer mechanism is an innovative design by doctor Zhou's technical engineering team (blade pile Group Pty Ltd, Qld, Australia).

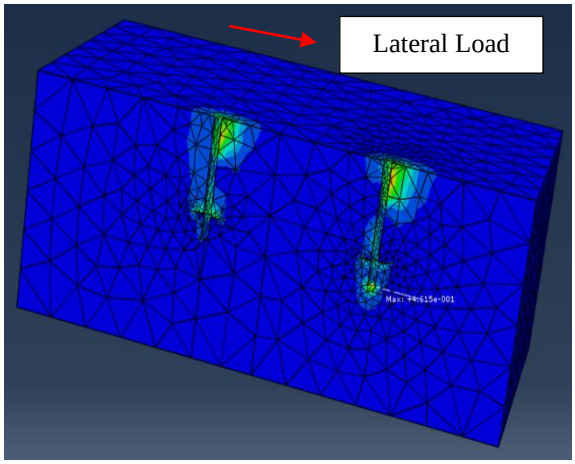

Fig. 3 Transferred lateral stress from An55.

The top displacement from the system as well as the maximum soil lateral movement of each model is determined by applying the same lateral loads, and it is summarized in Figure 4. From this figure, two tangent lines can be found from each curve, so the intersection of 75º is determined as the "yielding angle", which represents that the pile-ground angle can be selected from 50º to 74º, and when the angle is equal or greater than 75º, there will be dramatic displacement increasing from frame and soil.

For research purposes, the tested A-frame blade pile system considered the maximum frame leg-to-ground angle of 75º and for the real design, the optimum angle of 70º is recommended.

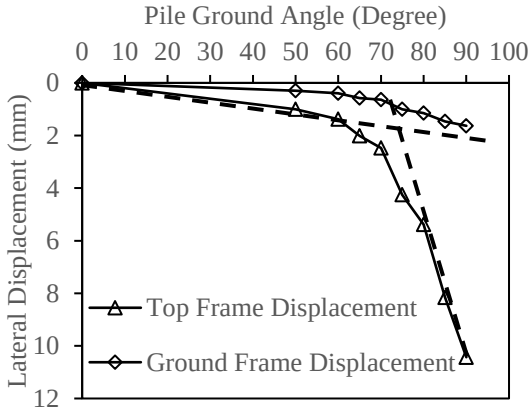

Fig. 4 Top Frame and Ground Soil Displacement.

4. FIELD TEST OF LATERAL LOAD A-FRAME SYSTEM

4.1 Geotechnical condition

To determine the subsurface geotechnical condition, the Dynamic Cone Penetrometer (DCP) test is conducted, and soil sampling is performed. Based on the statement of AS 1289. 6.3.2, and as shown in Figure 5, the drop numbers Np are recorded when the cone reaches 300 mm penetration (by 9 kg cone dropping 510 mm). As shown in Figure 6, the solid stem auger is used for the sampling. Moreover, different soil layers are also classified This boring terminated at 3 m below the ground surface.

Fig. 5 DCP Test of Site.

Fig. 6 Soil Auger Sampling.

For the 0.8-1 m drilling, the firm and stiff clay with sand are discovered; and the second layer of medium to dense sand is discovered at the depth of 1 to 1.5 m; the third layer is discovered as greycolorr clay with high plasticity. By using a pocket penetrometer, the average Cu for the first and third clay is determined as 50, and 100 kPa, respectively.

4.2 Description of A-frame System

The prepared piles are embedded in 1 meter. These two piles are all welded with a layer of blades, the blade side length is selected to be 250 mm with a wall thickness of 8mm.

As shown in Table 1, each element of the A-frame blade pile system is summarized. In this table, the thickness of the frame, as well as the piles, are 3 and 2.3 mm, respectively, and all these elements are made of steel with the same grade of 450 MPa.

Table 1 Field test parameters of A-frame system

Type	L	Embedment	Wall Thickness	Steel Grade
unit	m	m	mm	MPa
BP 1	1.3	1	2.3	450
BP 2	1.3	1	2.3	450
Frame 1	1.2	N/A	3	450
Frame 2	1.2	N/A	3	450

4.3 Test set-up

The assembled A-frame system is shown in Figure 7, which consists of a BHA bracket (used for the installation of torque tube connected with solar panel); two frame legs, and two blade piles. A load cell with a capacity of 3000 kg is used for recording the loads and three dial gauges are installed for the displacement measurement.

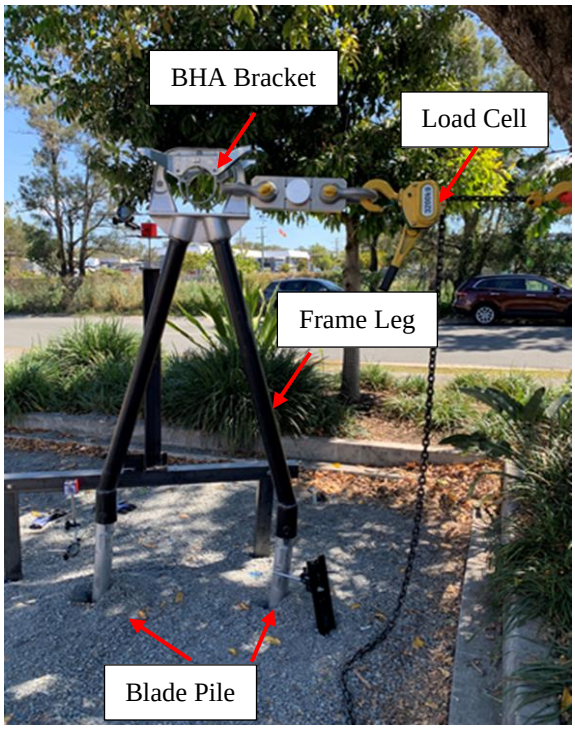

Fig. 7 A-frame System and Test Set up.

As can be seen in Figure 8, one dial gauge is installed from the Top Bearing Plate. For the pile head movement, the dial gauges are installed 200 mm above the ground as shown in Figure 9.

To perform the ultimate loading test, and acquire system behavior under wind load action, add 0.5 kN loads during loading stages, and release 2 to 4 kN during unloading stages. The dial gauge reading, as well as the load cell reading, are simultaneously recorded after the loads being added and released at time intervals of 2 to 5 minutes, respectively.

Fig.8 Top Plate Displacement Measurement.

Fig. 9 Pile Head Measurement.

5. NUMERICAL SIMULATION OF A-FRAME SYSTEM

The onsite test is also simulated as shown in Figure 10. The Mohr-coulomb constitutive

relationship is selected in the FEM model, and the elastic, as well as plastic behaviour of steel material, is set in the simulation. The steel parameters of Young's modulus, Poisson's ratio, yield and ultimate strength of steel are selected based on the material in the market as shown in Table 2.

Also, the soil strength parameters of cohesion (30kPa) and friction angle (37°) are used based on the interpreted values from in-situ soil testing. Further, the unit weight is also determined to be 19kN/m^3.

Table 2 Steel parameters in FEM.

Young's modulus	Poisson's ratio	Yield	Ultimate strength
MPa	N/A	MPa	MPa
210000	0.3	450	560

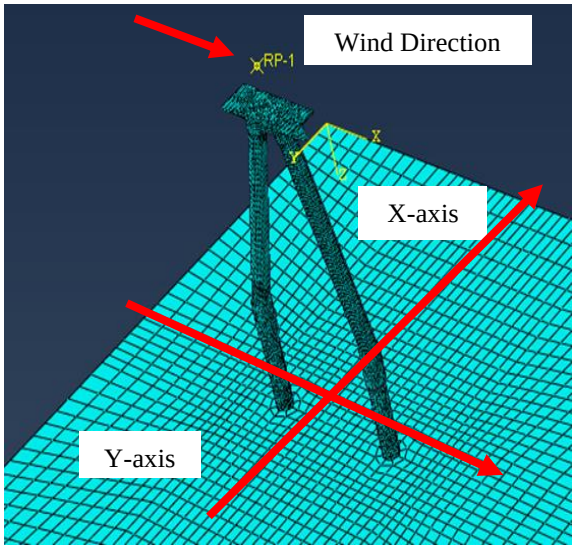

Fig. 10 A-frame Design in FEM Model.

The model considers two steps which include the geostatic as well as general static (target load calculation), and the interaction between the surfaces is defined as Hard contact in the normal direction (no penetration). As for the tangent direction, the penalty function is used to represent the friction between two surfaces.

The soil boundary is fully restrained, and the model is requested to calculate the corresponding loads when lateral top displacement achieves 200 mm (maximum lateral displacement observed onsite test). Note that, the diagram of the load versus top movement of the system is provided in the following section after the presentation of onsite test results.

6. RESULT AND DISCUSSION

6.1 Performance of A-frame system

The lateral loads are applied from left to right as shown in Figure 11. After the cycling loads are released, the top permanent displacement is around 131 mm, and two piles moved from left to right. It is obvious to see the gaps between soil and pile shaft being existed.

These two gaps, or soil permanent lateral movement from the left blade pile and right blade pile are discovered as 71.52 and 73.6 mm, respectively.

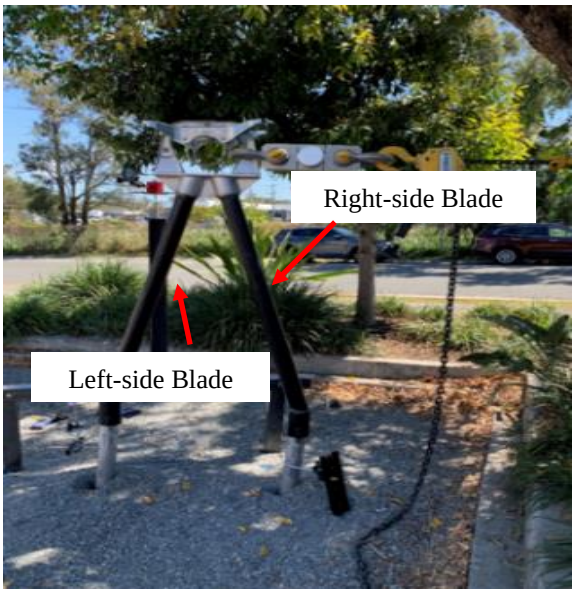

Fig. 11 System Test Performance.

Also, soil heave is observed. Figure 12 shows the A-frame pinned connection, which illustrates the frame rotated about the bolt. It is worth noting that the rotation of the sleeve tube (Figure 12) with respect to the pile tube is anticlockwise.

Fig. 12 A-frame Connection Behaviour.

The left and right blade piles after removing them from the soil are shown in Figures 13 and Figure 14, respectively. The right-side blade pile tube bent and there was slight deformation from the right pile blade.

Overall, the A-frame system rotated clockwise when lateral loads were applied from the frame top, and these two piles pushed the ground soil moving from left to right. The maximum bending moment occurred at the right pile below the ground surface about 300 mm.

Fig. 13 Left-side Blade Pile Performance.

Fig. 14 Right-side Blade Pile Performance.

6.2 Field test result

The lateral displacement of the left pile, right pile as well as top frame versus the applied loads are plotted in Figures 15 to 17. As shown in Figure 15, the total lateral displacement is observed as 38.27 mm under loading of 10.35 kN, and the permanent displacement is discovered as 21.28 mm after the first cycling loads being released.

The elastic displacement of this left pile is determined as 16.99 mm. Also, it shows that the total lateral displacement is observed as 93.62 mm under loading of 16.20 kN, and the permanent displacement is discovered as 71.52 mm after the second cycling load is released.

Two tangent lines can be found as shown in Figure 15, and the lines' intersection showing corresponding loads of 14.5 kN represents the "yielding" state. In detail, when loading beyond 14.5 kN, the soil displacement increase rate (Δdisplacement/Δload) will be higher.

This figure obviously shows that the soil displacement increases dramatically with a small loading increment after 14.5 kN. Thus, 14.5 kN can be determined as the ultimate bearing capacity of the left pile.

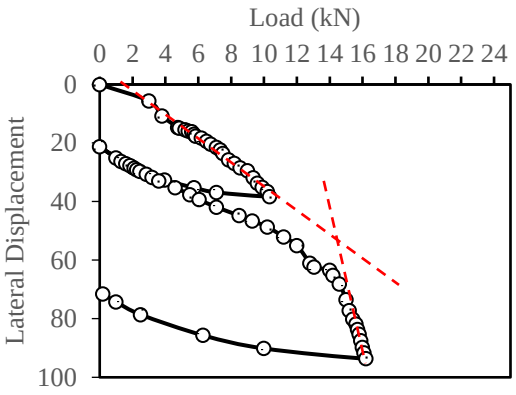

Fig. 15 Load versus Lateral Displacement of Left Blade Pile.

As shown in Figure 16, the lateral soil movement or right pile displacement behaves similar to the left blade pile. For the first cycling loading and unloading stages, the total, permeant displacement is discovered as 30.83 and 15.04 mm, respectively; and for the second cycling stage, the total and plastic deformation is 100.39 and 73.69 mm, respectively. The plotted Figure 16 also shows two tangent lines. By finding the intersection

between two tangent lines, the ultimate bearing capacity of the right pile is determined as 13.2 kN.

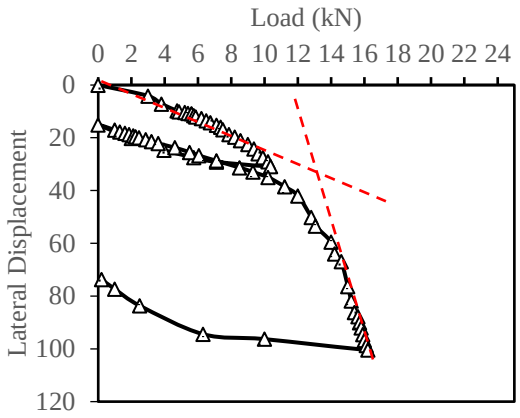

Fig. 16 Load versus Lateral Displacement of Right Blade Pile.

Under two cycling loads, the lateral load versus the top frame displacement is shown in Figure 17. The maximum total displacement from the first and second loads are determined as 77.12 and 186.3 mm, respectively. Again, there are two tangent lines being found, with an intersection value of 13.8 kN. This value can be decided as the ultimate bearing capacity of the standard A-frame blade pile system under firm to stiff geotechnical conditions.

To make the conservative design, the A-frame ultimate capacity can be determined as the smallest value, which is 13.2 kN. From a practical point of view, when the frame is subjected to 13.8 kN, there is no evident displacement increase, thus taking 13.8 kN as the ultimate bearing capacity is acceptable.

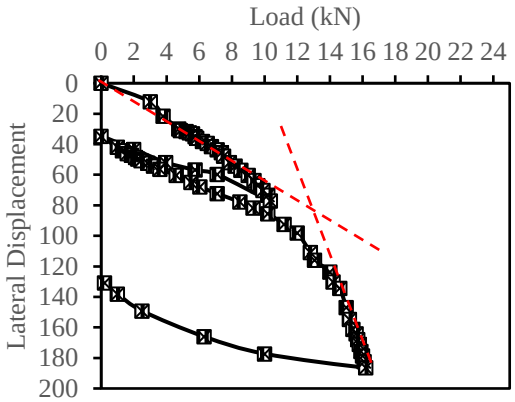

Fig. 17 Load versus Lateral Displacement of A-frame System.

6.3 Interpretation of the SLT

For the data obtained on site, there is another way to obtain the ultimate bearing capacity analytically. By plotting the Nominated Displacement Gradient (applied loads over displacement) as shown in Figure 18, 3 best-fit lines which mathematically show the capacity trends of the left and right blade pile, as well as the system, are illustrated in the diagram.

Assume the applied loads are infinitely equal to zero, whereas the displacement increases to infinity, the value of Load/displacement will close to zero, and the corresponding loads will be the intersection between the best fit line in Figure 18 and the y-axis. Note that, this load is the analytical capacity or semi-empirical capacity based on the interpretation of the field test data.

The function showing the analytical capacity trend of left, and right blade piles and frames are also given in Figure 18, and when x equals zero, the capacity is determined as 24.602, 20.492 and 26.128 kN, respectively. Since this method is the mathematical method, the smallest value among the left and right blade piles, and the frame are considered as the ultimate lateral capacity. In this context, the capacity of the A-frame blade pile system is 20.49 kN.

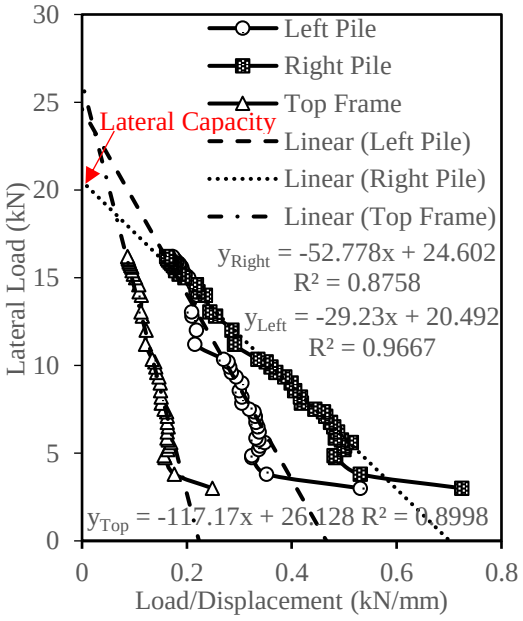

Fig. 18 Nominated Displacement Gradient.

6.4 FEM Simulation of the Field Test

The behaviour of A-frame blade pile system under lateral wind load action is obtained by FEM simulation as shown in Figure 19. As shown in this figure, it shows the lateral displacement of each element including soil. It can be clear to see that the maximum displacement is observed from the upper bracket location.

Moreover, for the soil displacement, the maximum soil lateral movement is discovered from the right side of two piles. Also, the disturbed soil is mostly discovered near the piles within the range of 2 D (D: Pile distance).

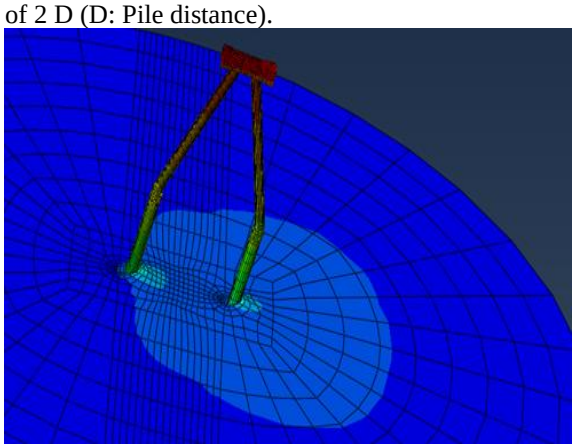

Fig.19 Lateral Wind Load Action of A-frame Blade Pile System.

To simulate the real onsite testing process, the 200 mm displacement is set as a controlled displacement in FEM, because the applied loads onsite had led to 200 mm top movement. The corresponding loads to be applied from the reference point (top of bracket) when the top bracket moves from 0 to 200 mm is obtained by FEM simulation, and this data is plotted in Figure 19.

As shown in Figure 20, the maximum applied load is discovered as 14.16 kN which is less than the maximum loads applied onsite (16.2 kN), which represents that the FEM will provide a relative conservative result. By finding two tangent lines from FEM load-displacement curve, the ultimate bearing capacity is discovered as 12 kN.

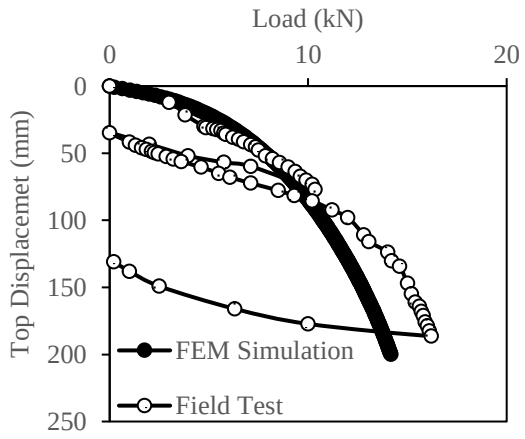

Fig. 20 The Corresponding Loads of Top Bracket.

7. CONCLUSION

This paper presents the onsite test of A-frame blade pile system as well as the FEM simulation. The behaviour of this A-frame system is observed. Further, the field test data is collected and analyzed. The conclusions are summarized as follows:

1. The left and right blade pile foundations have different loading capacities. By finding two tangent lines in Load-displacement curves, they are 14.5 and 13.2 kN respectively, and by interpretation of the field data, the analytical capacity is 24.6 kN and 20.5 kN, respectively.
2. The reason for the above finding is that these two piles' mechanical behaviour is different. The left pile is subjected to the "pull out" action, whereas the right pile is subjected to the "push in" effect.
3. The mechanical behaviour of soil is found in this research. It is discovered that the soil near the ground surface will resist the transferred stress from the top frame, and laterally move. Also, the soil below the blades from the right pile foundation resists the stress, whereas the soil above the blades from the left pile foundation resists the transferred stress simultaneously.
4. From a practical point of view, 13.8 kN is the ultimate bearing capacity of the A-frame when the geotechnical condition is firm to stiff soil material. And the analytical capacity of A-frame is 20.5 kN for the A-frame system.
5. The FEM result provided very close behaviour of soil and A-frame blade pile system, and the ultimate bearing capacity of the system is determined as 12 kN. Furthermore, the FEM simulation can provide conservative results.

8. RECOMMENDATION AND FUTURE STUDY POTENTIALS

For this ultimate load test, the standard blade pile tube bend, this is due to the designed tube thickness (2.3 mm) and blade size being small. These blades will not have enough contact area to work with soil when designing larger wind load action. Moreover, the soil exploration of some locations shows blow count of 3 and some shows 8 at the same depth, therefore, the onsite test geotechnical condition may not be accurate.

In this context, further research will be focused on the blade and pile dimension influence on system capacity, and more accurate soil exploration is required.

Currently, sustainable development has become an important development direction. Solar

installations can reduce the emission of pollutants. A-frame blade pile system can improve the energy collection efficiency of solar panels and produce more energy. Studying the A-frame blade pile system can better improve the range of applications of solar panels. Thus, promoting the development of clean energy.

9. REFERENCES

[1] Zhou J.L. and Erwin Oh., Full-Scale Field Tests of Different Types of Piles: Project-Based Study Springer Nature, Zhejiang, China, 2021, Vol. 62, pp.1-272.

[2] Mokwa R.L. and Duncan J.M., Experimental evaluation of lateral-load resistance of pile caps. Journal of Geotechnical and Geoenvironmental Engineering, 2001, Vol. 127, Issue 2, pp. 185-192.

[3] Zhao H.Y., Liu X.L., Jeng D.S., Zheng J.H., Zhang J.S. and Liang Z.D., Numerical investigation into the vulnerability to liquefaction of an embedded pipeline exposed to ocean storms. Coastal Engineering, Vol 172, Issue 14, 2022, pp.1-16.

[4] Perko H.A., Helical piles: a practical guide to design and installation. John Wiley & Sons, Hoboken, New Jersey, 2009, pp.1-512.

[5] Trofimenkov J.G. and Maruipolshii L.G., Screw piles used for mast and tower foundations. In: Proceedings of the 6th Int. Conf. on Soil Mechanics and Foundation Engineering, Vol. 2, Issue 0, 1965, pp. 328–332.

[6] Mitsch M.P. and Samuel P.C., Uplift Capacity of Helix Anchors In Sand., Unknown Host Publication Title, American Society of Civil Engineers (ASCE), 1985, pp.26-47.

[7] Mooney J.S., Stephan A. and Samuel P.C., Uplift Capacity of Helix Anchors In Sand and Silt., Unknown Host Publication Title, American Society of Civil Engineers (ASCE), 1985, pp. 48-72.

[8] Mohajerani A., Bosnjak D. and Bromwich D., Analysis and Design Methods of Screw Piles: A Review. Soils and Foundations, Vol. 56, Issue 1, 2016, pp. 115–128.

[9] Vignesh V. and Muthukumar M., Design parameters and behaviour of helical piles in cohesive soils—A review. Arabian Journal of Geosciences, Vol. 13, Issue 22, 2020, pp. 1-14.

[10] Feng S.J., Fu W.D., Chen H.X., Li H.X., Xie Y.L., Lv S.F. and Li J., Field Tests of Micro Screw Anchor Piles Under Different Loading Conditions at Three Soil Sites, Bulletin of Engineering Geology and the Environment: The Official Journal of the Iaeg, Vol. 80, Issue. 1, 2021, pp. 127–144.

[11] Xu Y., Li J., Tan Q., Peters A.L. and Yang C., Global status of recycling waste solar panels: A review. Waste Management, 2018, Vol. 75: Issue 43, pp. 450-458.

[12] KYODO. Wild winds cause damage, injury in Gunma. The Independent Voice in Asia, Jun 16, 2015.https://www.japantimes.co.jp/news/2015/06/16/national/wild-winds-cause-damage-injury-gunma.

[13] Agarwal A., Irtaza H. and Khan M.A., Experimental Study of Pulling-Out Capacity of Foundation for Solar Array Mounting Frames. Indian Geotechnical Journal, Vol. 51, Issue. 2, 2021, pp. 414–420.